A facile and general approach to polynary semiconductor nanocrystals via a modified two-phase method

2011 Nanotechnology 22 245605

(http://iopscience.iop.org/0957-4484/22/24/245605)

Nanotechnology **22** (2011) 245605 (8pp) doi:10.1088/0957-4484/22/24/245605

A facile and general approach to polynary semiconductor nanocrystals via a modified two-phase method

Xiuying Wang[1], **Zaicheng Sun**[1,3], **Cong Shao**[1], **Daniel M Boye**[2] **and Jialong Zhao**[1]

[1] Key Laboratory of Excited State Processes, Changchun Institute of Optics, Fine Mechanics and Physics, Chinese Academy of Sciences, 3888 Eastern South Lake Road, Changchun 130033, People's Republic of China
[2] Physics Department, Davidson College, Davidson, NC 28035, USA

E-mail: sunzc@ciomp.ac.cn

Received 16 January 2011, in final form 29 March 2011
Published 21 April 2011
Online at stacks.iop.org/Nano/22/245605

Abstract

Cu_2ZnSnS_4 nanocrystals were synthesized through a modified two-phase method and characterized with transmission electron microscopy (TEM), powder x-ray diffraction (XRD) and UV–vis spectroscopy. Inorganic metal salts were dissolved in the polar solvent triethylene glycol (TEG) and then transferred into the non-polar solvent 1-octadecene (ODE) by forming metal complexes between metal ions and octadecylamine (ODA). Since nucleation and growth occur in the single phase of the ODE solution, nanocrystals could be produced with qualities similar to those obtained through the hot-injection route. Balancing the reactivity of the metal precursors is a key factor in producing nanocrystals of a single crystalline phase. We found that increasing the reaction temperature increases the reactivity of each of the metal precursors by differing amounts, thus providing the necessary flexibility for obtaining a balanced reactivity that produces the desired product. The versatility of this synthesis strategy was demonstrated by extending it to the production of other polynary nanocrystals such as binary (CuS), ternary ($CuInS_2$) and pentanary ($Cu_{2-x}Ag_xZnSnS_4$) nanocrystals. This method is considered as a green synthesis route due to the use of inorganic metal salts as precursors, smaller amounts of coordinating solvent, shorter reaction time and simpler post-reaction treatment.

S Online supplementary data available from stacks.iop.org/Nano/22/245605/mmedia

(Some figures in this article are in colour only in the electronic version)

1. Introduction

Copper-based chalcopyrite materials have attracted increasing attention due to their potential applications in high efficiency and low cost thin film solar energy harvesting devices [1–11]. These materials show favorable light absorption properties such as a tunable bandgap (1.0–1.7 eV) and a high absorption coefficient ($>10^4$ cm^{-1}). As a representative of second-generation solar cells, copper-based chalcopyrite thin film solar cells have demonstrated high power conversion efficiency (PCE). For example, $Cu(In_xGa_{1-x})Se_2$ (CIGS) thin film solar cells exhibit PCE of up to 20% [4, 5]. Brauger *et al* fabricated $CuInS_2$ thin film solar cells with PCE of 11.4% [6, 7]. Cu_2ZnSnS_4 (CZTS) photovoltaic devices have been made with PCE of up to 6.7% [8]. However, high fabrication cost is still a significant barrier for the practical application of this class of materials. Currently, these thin film solar cells are primarily fabricated by co-evaporation deposition [4, 9], sputter deposition [10], spray pyrolysis [11, 12] and electrodeposition [13] techniques. All of these techniques utilize restrictive fabrication processes, for example, vacuum and/or high temperature technologies.

Non-vacuum solution processing has been considered as an alternative route, since the precursor particle solution could

[3] Author to whom any correspondence should be addressed.

be easily coated onto a substrate and sintered into bulk material for printed and flexible photovoltaic devices [14–16]. Further, colloidal nanocrystals could be an important alternative for solution processing even without a sintering step because the nanocrystals are already in the crystalline phase [17]. To this end, colloidal Cu-based nanocrystals (Cu_2S, $CuInS_2$, $CuInSe_2$, CIGS, CZTS) have recently been extensively investigated [18–29]. Among Cu-based materials, CZTS is nontoxic and its elements are more abundant in nature in comparison with CIGS. Due to these special properties, CZTS is considered a promising material for application in low cost and environmentally friendly thin film solar cells. A few groups [26–28] have reported the synthesis of CZTS nanocrystals through the hot-injection method using organometallic compounds as precursors in coordinating solvents. However, there remains a need to develop a simple and practical synthesis route that is more readily scaled before there is practical use of these materials in commercial products or devices.

In general, nanocrystals are obtained through two strategies: (1) a hot-injection method, which contains a burst nucleation with subsequent separation of nucleation and growth [30], and (2) a two-phase method, which possesses prolonged nucleation and growth processes [31]. In a hot-injection synthesis route, most semiconductor nanocrystals are obtained by using extremely expensive, unstable and hazardous precursors. Also, a large amount of coordinating solvent such as organic amine or phosphine is utilized as ligands and solvent. In a two-phase method, the simple cationic and anionic precursors are dissolved in the organic and aqueous phases. Nucleation and nanocrystalline growth occur only at the interface of the organic and aqueous solutions. In this case, diffusion-controlled growth results in the formation of nanocrystals with a narrow size distribution and a very lengthy growth time. From the viewpoint of green chemistry, the two-phase method is considered to be a more favorable route because smaller amounts of coordinating solvent and simple metal salts are used in the reaction [32]. The two-phase method was originally used to synthesize gold nanoparticles [33], and then extended to monodispersed noble metal, oxide, semiconductor, alloy and core/shell structure nanoparticles [34–38]. To the best of our knowledge, only binary nanocrystals have been synthesized through the two-phase method. There is no report on the synthesis of ternary, quaternary and pentanary semiconductor nanocrystals through the two-phase method due to the difficulty of obtaining a pure product.

Here we have developed a facile and 'greener' route for synthesizing quaternary CZTS nanocrystals through a modified two-phase method. In addition, we have found that this method can be applied to the synthesis of polynary (binary, ternary and pentanary) nanocrystals. Due to the immiscibility of the polar solvent triethylene glycol (TEG) and non-polar solvent 1-octadecene (ODE), a two-phase reaction system was developed to synthesize CZTS nanocrystals. In this reaction, inorganic metal salts are dissolved in TEG and then transferred into ODE through a phase transfer agent octadecylamine (ODA). Since the nucleation and growth of nanocrystals occur within the ODE microdroplet phase, the quality of the resulting nanocrystals is similar to that of nanocrystals obtained from a hot-injection route. This new strategy possesses the following advantages: (1) lower cost by utilizing inorganic metal salts that are relatively inexpensive and easily obtained as starting materials; (2) significant reduction by an order of magnitude in the amounts of solvents used in purification; (3) direct recycling of the polar solvent in future reactions; (4) significant reduction in reaction time compared to the traditional two-phase method; and (5) the ability to synthesize and leverage new polynary semiconductor nanocrystals.

2. Experimental section

2.1. Materials

Octadecylamine (ODA, 95%) was purchased from Alfa Aesar. 1-octadecene (ODE) was purchased from Aldrich. Sulfur powder (99.99%) and triethylene glycol (TEG), copper chloride ($CuCl_2{\cdot}2H_2O$), zinc acetate ($Zn(Ac)_2{\cdot}2H_2O$), tin chloride ($SnCl_2{\cdot}2H_2O$), silver nitrate ($AgNO_3$) and indium nitrate ($In(NO_3)_3{\cdot}4.5H_2O$) were purchased from Beijing Chemical Reagent Company. All chemicals were used without further purification.

2.2. Preparation of CZTS nanocrystals (see supplementary material for protocols of other nanocrystals available at stacks.iop.org/Nano/22/245605/mmedia)

In a typical reaction, 0.5 mmol (85.2 mg) of $CuCl_2{\cdot}2H_2O$, 0.25 mmol (54.8 mg) of $Zn(Ac)_2{\cdot}2H_2O$ and 0.25 mmol (56.4 mg) of $SnCl_2{\cdot}2H_2O$ were added to 30 ml of TEG in a 50 ml three-necked flask on a Schlenk line. The reaction mixture was degassed under Ar for 30 min at 140 °C, followed by heating to 220 °C. 1.5 mmol (50 mg) of sulfur powder was dissolved in 2 ml of ODE, combined with 500 mg of ODA and then rapidly injected into the hot metal precursor solution. The solution turned black immediately. The reaction was maintained at 220 °C for 1 h to obtain high quality crystalline nanocrystals. The heating mantle was then removed and the reaction vessel was allowed to cool to room temperature naturally without stirring. The reaction solution spontaneously separated into two layers, the top black ODE layer and the bottom transparent TEG layer (see Sfigure 1 in the supplementary data available at stacks.iop.org/Nano/22/245605/mmedia). The TEG layer was removed with pipettes and could be directly used for a new batch. 3–5 ml of ethanol was added to the ODE solution and this mixture was centrifuged at 6000 rpm for 5 min. The clear supernatant was discarded and its precipitate was redispersed in 3 ml of chloroform. The nanocrystals were washed two more times with ethanol and chloroform. The final product could be redispersed in typical organic solvents such as chloroform, toluene and hexane.

2.3. Characterization of the nanocrystals

Powder x-ray diffraction (XRD) measurements were performed in a Rigaku XRD spectrometer with a Cu Kα line of

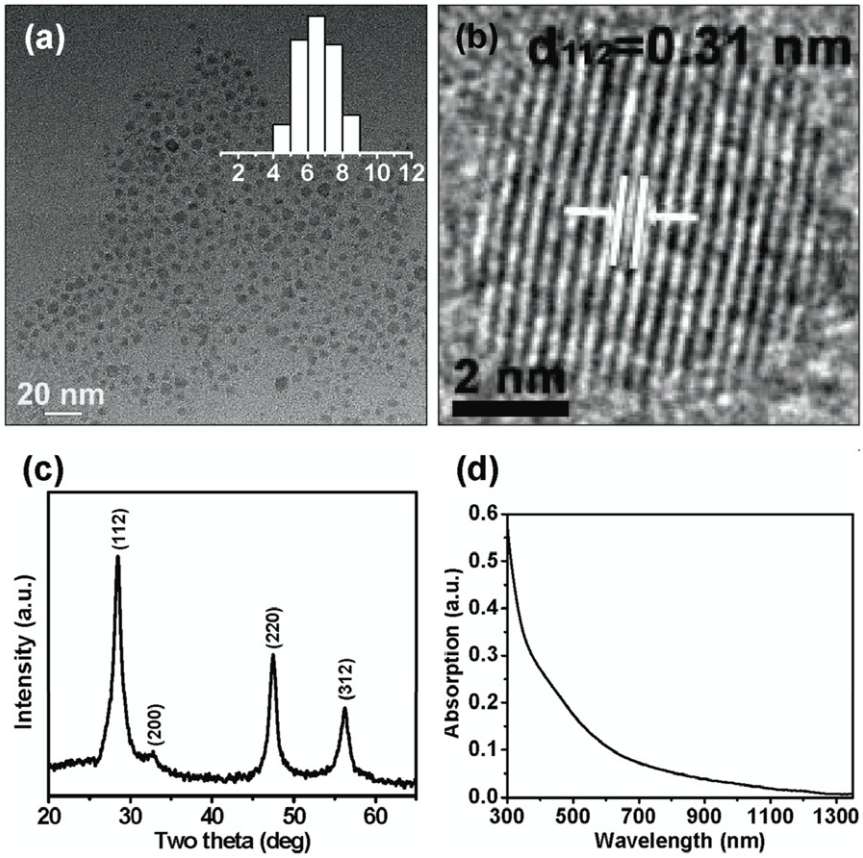

Figure 1. (a) Low magnification TEM image, inset is a histogram of nanocrystal size distribution, (b) HRTEM image, (c) XRD pattern and (d) absorption spectrum of Cu_2ZnSnS_4 nanocrystals synthesized by a modified two-phase method.

0.154 nm. Transmission electron microscope (TEM) pictures were obtained using an FEI Tecnai G2 operated at 200 kV. TEM samples were prepared by drop-casting nanocrystals dispersed in hexane onto carbon-coated 200 mesh copper TEM grids. Scanning electron microscope (SEM) images and energy-dispersive x-ray spectroscopy were measured on a JEOL JSM 4800F. The SEM samples were prepared by drop-casting the nanocrystals in hexane onto a silicon wafer. The UV–vis absorption spectra were recorded on a UV-3600 UV–vis–NIR scanning spectrophotometer (Shimadzu). The nanocrystal solutions were prepared in chloroform using a quartz cuvette with a 1 cm path length. The Raman spectrum was obtained on a laser Raman spectrometer (LabRam Infinity) with the 488 nm excitation line of an Ar^+ laser at room temperature.

3. Results and discussion

In the synthesis of CZTS nanocrystals, inorganic metal salts ($CuCl_2$, $Zn(Ac)_2$ and $SnCl_2$) are dissolved in the polar solvent TEG; sulfur powder and ODA are dissolved in the non-polar solvent ODE. TEG is chosen as the polar solvent because it has a high boiling point (286 °C) and can dissolve the inorganic salts, whereas ODE has a boiling point of 314 °C and can dissolve the sulfur powder. Thus the two immiscible solvents TEG and ODE form a two-phase reaction system with a relatively high boiling point. In the reaction ODA has multiple functions. First, it works as a phase transfer agent to transfer the metal ions from the polar solution into the non-polar solution through the formation of complexes of metal ions and ODA. Second, ODA acts as a capping agent that stabilizes the nanocrystals in the ODE solution, keeping them from aggregating in the solution. Finally, ODA depresses the reactivity of the metal ions to some degree due to the formation of metal–ODA complexes. When the S, ODA/ODE solution was added to the TEG solution under vigorous stirring, the ODE solution was broken into microdroplets and dispersed into the TEG solution. Metal–ODA complexes rapidly form at the interface of ODE/TEG and the metal ions were transferred into the ODE solution. With continuous transfer of the metal ions into the ODE solution, the CZTS nanocrystals grow in diameter.

The size, morphology and optical properties of the CZTS nanocrystals were characterized by TEM, XRD and UV–vis spectroscopy. Typical results are shown in figure 1. Figure 1(a) shows a TEM image of CZTS nanocrystals with an average size of 6.5 ± 1.0 nm, calculated over 100 nanoparticles from the TEM image. A high-resolution TEM (HRTEM) image (figure 1(b)) clearly shows the highly crystalline nature of the CZTS nanocrystals. The lattice fringe, with interplanar spacing of 0.31 nm, agrees well with the interplanar spacing of the (112) crystal plane. XRD peaks at 28.5°, 32.9°, 47.3° and 56.1° (figure 1(c)) could be assigned to the (112), (200), (220)

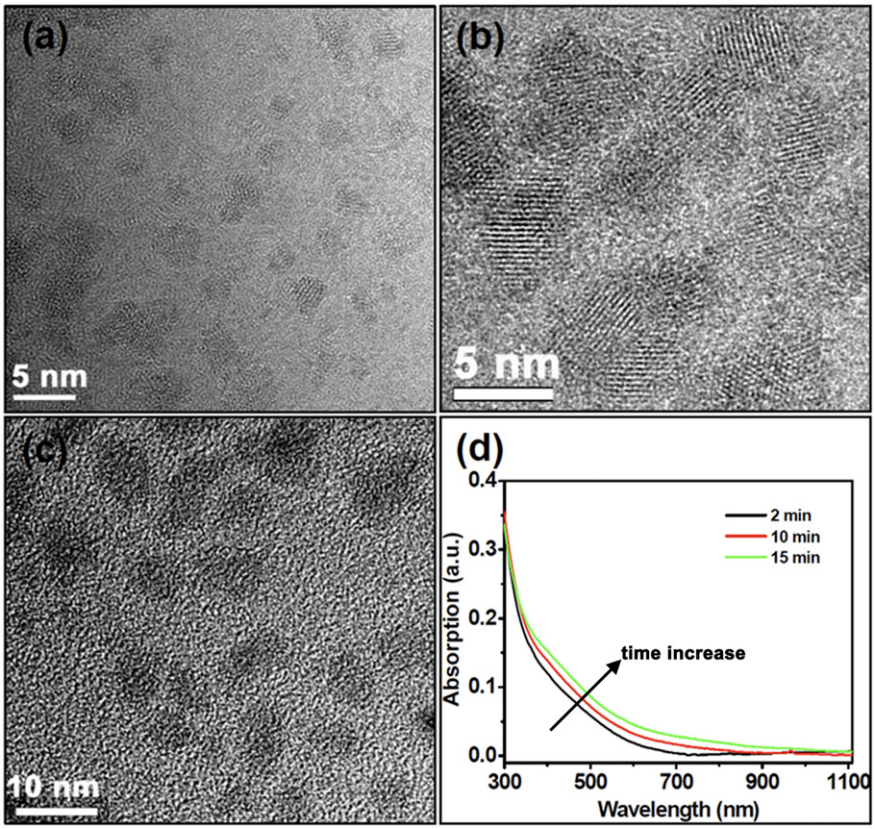

Figure 2. TEM images of Cu_2ZnSnS_4 nanocrystals prepared for (a) 2 min, (b) 10 min and (c) 15 min, respectively, and (d) their absorption spectra.

and (312) planes of the kesterite structure (JCPDS no. 26-0575) [27, 28]. Since the XRD pattern of CZTS nanocrystals is very similar to that of ZnS, Raman spectroscopy was further used to confirm the component of our samples. According to Fernandes' report, the three major Raman peaks of CZTS are located at 338, 288 and 257 cm^{-1} [39]. The Raman peaks of ZnS appear at 350 and 275 cm^{-1} [40]. Sfigure 2 in the supplementary data (available at stacks.iop.org/Nano/22/245605/mmedia) shows the Raman spectrum of our CZTS nanocrystals. It can be clearly seen that there is only a broad peak appearing at 338 cm^{-1} and no significant peak at 350 or 275 cm^{-1}, indicating that pure CZTS nanocrystals were obtained. The average composition of the nanocrystals determined by energy-dispersive x-ray spectroscopy (EDS) was $Cu_{2.73}Zn_{0.6}Sn_{1.14}S_{3.86}$. The nanocrystals are copper-rich and zinc-deficient. This may be related to the higher reactivity of copper, resulting in occupying some sites of zinc in the kesterite structure [27]. The UV–vis absorption spectrum of the CZTS nanocrystals (figure 1(d)) displays a strong response in the visible region with an estimated optical bandgap of 1.50 eV, consistent with a previous report [27].

In order to understand the reaction mechanism, samples were removed at different periods during the reaction. Figures 2(a)–(c) present TEM images of CZTS nanocrystals prepared for 2, 10 and 15 min, respectively. For 2 min, the nanoparticles with sizes of 2–3 nm have formed in the solution. XRD analysis confirms that the nanoparticles are pure CZTS nanocrystals in the kesterite phase even at this early stage (Sfigure 3 in the supplementary data available at stacks.iop.org/Nano/22/245605/mmedia). This indicates that the nucleation of CZTS nanocrystals occurs as the metal ions are transferred into the ODE phase and the reactivity of metal ions reaches a balance. The size of nanocrystals increases to 4–5 nm for 10 min and ∼7 nm for 15 min, respectively. This demonstrates the size of nanocrystals is limited by the transfer rate of metal ions into the ODE phase. With an increase in reaction time, more metal ions are transferred into the ODE solution and larger nanocrystals are obtained. The size of the nanocrystals after 15 min is similar to that of nanocrystals after 1 h (figure 1(a)), indicating that all of the metal salts have transferred into the ODE solution and been consumed in the growth process within 15 min. Moreover, the average compositions of the above three samples are similar to those of the product prepared after 1 h. From absorption spectra (figure 2(d)), it can be seen that the edge of the absorption band is tunable in the region from 600 to 800 nm along with the increase in the size of the nanocrystals. It could be attributed to the size effect of the as-synthesized CTZS nanocrystals, since all these samples have a similar composition.

Based on the above results, a possible reaction process is proposed as shown in scheme 1. Inorganic Cu^{2+}, Zn^{2+} and Sn^{2+} salts are dissolved into the TEG solution. With injection of the S, ODA/ODE solution into the TEG solution under vigorous stirring, the ODE solution is immediately broken and forms numerous microdroplets in the TEG solution. The ODA, working as a phase transfer agent, rapidly forms metal–ODA

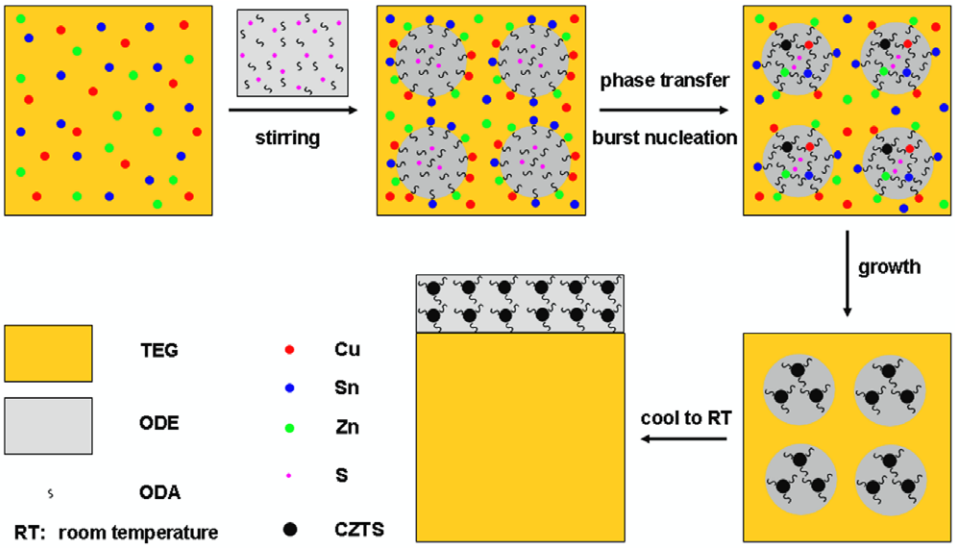

Scheme 1. The reaction process of Cu_2ZnSnS_4 nanocrystals via a modified two-phase method.

complexes with metal ions and transfers metal ions into the ODE solution. After that, the nucleation simultaneously takes place between metal complexes and sulfur in the ODE solution. This process is equivalent to the burst nucleation stage in the hot-injection method. After nucleation, metallic cations, which were transferred later, are mainly used for the growth process via diffusion-controlled transfer. The ODA also works as a capping agent for the nanocrystals and maintains the stability of nanocrystals in the ODE solution. Aggregates of CZTS were obtained when the reaction was carried out at 250 °C without ODA (Sfigure 4 in the supplementary data available at stacks.iop.org/Nano/22/245605/mmedia). The particles were formed at the interface between the ODE droplet and TEG and could not be dispersed in common solvents after treatment.

In the synthesis of $CuInS_2$ nanocrystals, the formation of Cu_xS ($x = 1$–2) nanophases was found to be inevitable when the solution was composed of indium and copper carboxylate precursors and a pure non-coordinating solvent (such as ODE), trioctylphosphine oxide, amines, carboxylic acid and their mixtures. Purity of the phase is an important evaluative parameter for the synthesis of polynary Cu-based nanocrystals. Balancing the reactivity of cationic precursors is one way to obtain single-phase nanocrystals in the final product. In general, metal ions have high reactivity that can be suppressed by the formation of metal complexes. In Xie's report [41], thiols were used as strong ligands to suppress the reactivity of copper in order to synthesize high quality $CuInS_2$ nanocrystals, since Cu complexes are more reactive than In complexes. In our case, CuS peaks were observed in the XRD pattern when the reaction temperature was 190 °C. This indicated that Cu–ODA complexes were more reactive than Zn–ODA and Sn–ODA complexes in the reaction. In order to obtain a single-phase product, lowering the reactivity of Cu–ODA complexes could be effective, as in Xie's route. Another possibility is to increase the reactivity of Zn–ODA and Sn–ODA complexes to reach a balance. In this paper, increasing the reaction temperature is utilized to adjust the reactivity of

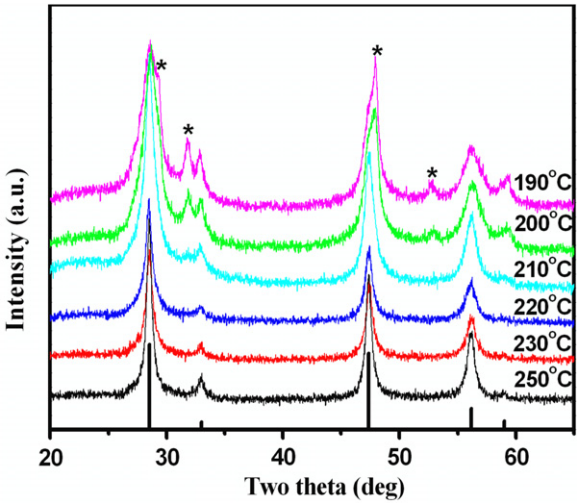

Figure 3. XRD patterns of Cu_2ZnSnS_4 nanocrystals obtained at different reaction temperatures. Peak marked with asterisk refers to CuS. The diffraction pattern of bulk Cu_2ZnSnS_4 is indicated for comparison.

the cation complexes (Zn and Sn). According to the XRD patterns, as shown in figure 3, the percentage of CuS in the final products decreases with the elevation of reaction temperature up to 220 °C. From a kinetics view, the reactivity of all cation complexes is increased through elevation of the reaction temperature. However, the relative increase in reactivity of Cu–ODA complexes is less than that of Zn–ODA and Sn–ODA complexes. When the reaction temperature is over 220 °C, the final product is a single kesterite phase of CZTS nanocrystals with similar size and no detectable amounts of CuS present. In addition, all these nanocrystals can also be redispersed in typical organic solvents such as chloroform, toluene and hexane.

This synthesis route was not only used for the preparation of quaternary CZTS nanocrystals, but also for synthesis

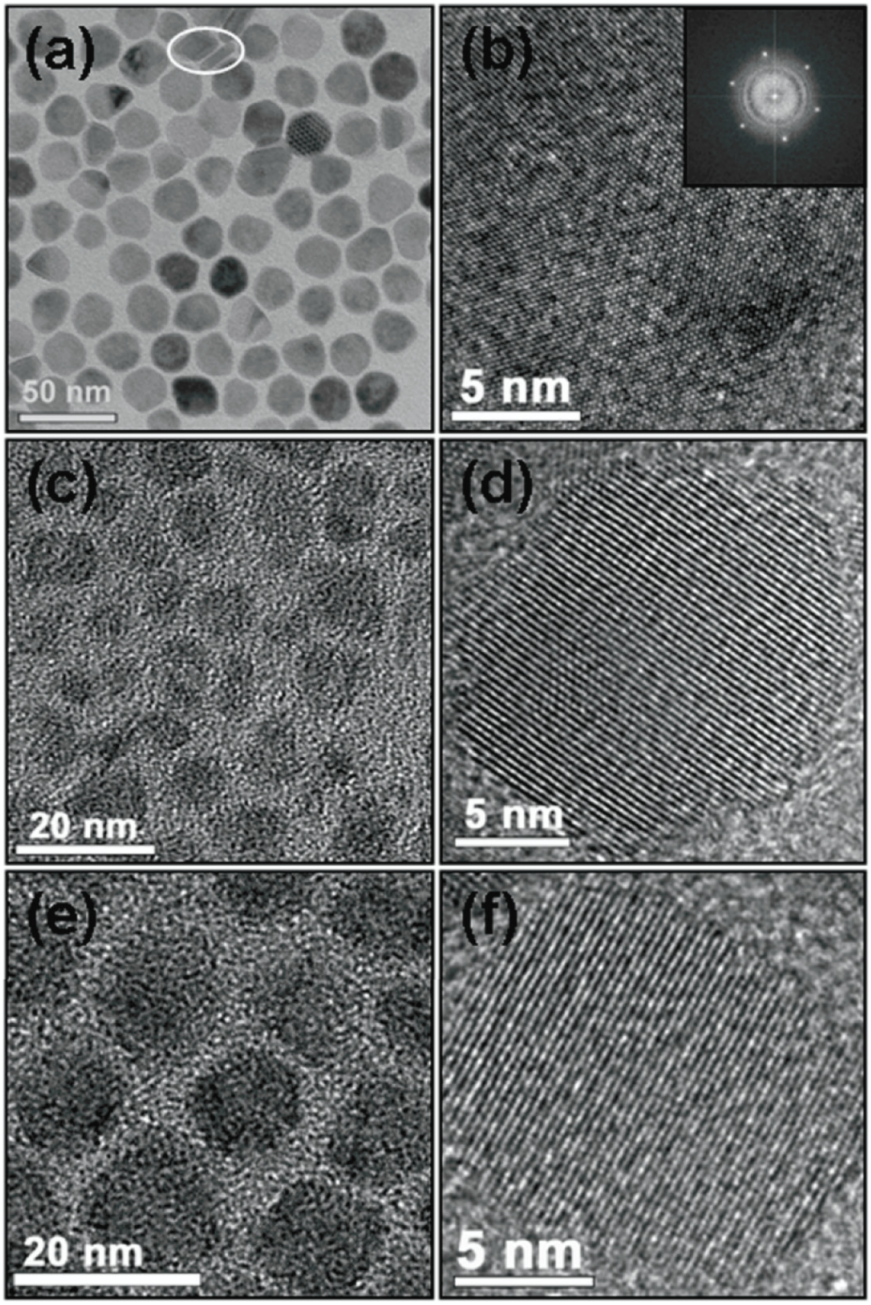

Figure 4. Low magnification TEM and HRTEM images of CuS ((a) and (b)), $CuInS_2$ ((c) and (d)) and $Cu_{2-x}Ag_xZnSnS_4$ ((e) and (f)) nanocrystals. The oval highlights the side view of CuS nanoplates. The inset of HRTEM (b) is the corresponding Fourier transform pattern.

of other binary, ternary and even pentanary semiconductor nanocrystals. Here, CuS, $CuInS_2$ and $Cu_{2-x}Ag_xZnSnS_4$ nanocrystals were chosen as examples. Figure 4 shows TEM results for binary, ternary and pentanary Cu-based chalcopyrite nanocrystals. As an example of binary nanocrystals, CuS quasi-hexagonal nanoplates (the side view of the nanoplates was circled in figure 4(a)) with ∼25 nm in diameter and ∼9 nm in thickness are obtained and are similar to those found in Du's report [22]. The HRTEM image shows highly crystalline nanoparticles. XRD peaks (figure 5, CuS pattern) fitted well to the hexagonal covellite CuS phase except for an additional small peak assigned to Cu_2S (marked with an asterisk). Ternary $CuInS_2$ nanocrystals were obtained at 260 °C through the two-phase method. Figures 4(c), (d) and 5, $CuInS_2$ pattern, show representative TEM images and an XRD pattern of $CuInS_2$ nanocrystals. All confirm that the nanocrystals are chalcopyrite and no other phase is produced in our reaction. Recently, Tsuji *et al* reported that $CuAgZnSnS_4$ nanocrystals, a promising low bandgap (1.4 eV) water-splitting agent, possessed relatively high photocatalytic activity [42]. $Cu_{2-x}Ag_xZnSnS_4$ nanocrystals were also synthesized through our method. A TEM image of $Cu_{2-x}Ag_xZnSnS_4$ nanocrystals with an average diameter of ∼20 nm is shown in figure 4(e). HRTEM (figure 4(f)) and XRD patterns (figure 5, $Cu_{2-x}Ag_xZnSnS_4$ pattern) are similar to those of CZTS nanocrystals, indicating only a small

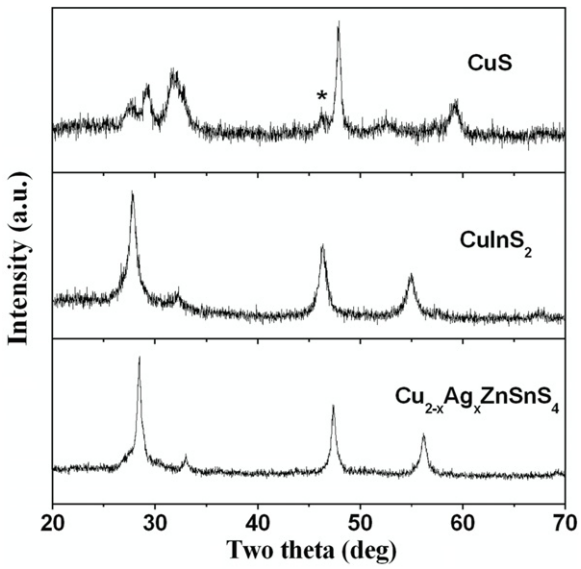

Figure 5. XRD patterns of CuS, $CuInS_2$ and $Cu_{2-x}Ag_xZnSnS_4$ nanocrystals. Peak marked with asterisk refers to Cu_2S.

amount of Cu is replaced. The ratio of Cu:Ag is approximately 4:1, determined by energy-dispersive x-ray spectroscopy (EDAX) analysis (EDAX spectra for all nanocrystals are shown in Sfigure 5 in the supplementary data available at stacks.iop.org/Nano/22/245605/mmedia). Based on the above results, the nanocrystals we obtained are considered to be $Cu_{2-x}Ag_xZnSnS_4$.

4. Conclusion

In summary, we have developed a facile and 'greener' synthesis route for Cu-based binary (CuS), ternary ($CuInS_2$), quaternary (Cu_2ZnSnS_4) and pentanary ($Cu_{2-x}Ag_xZnSnS_4$) nanocrystals through a modified two-phase method. Inorganic salts are directly used as precursors and are dissolved in the polar solvent TEG, whereas sulfur and ODA ligands are dissolved in the non-polar solvent ODE. The use of inexpensive precursors, non-coordinating solvent and a simple post-treatment make this route more environmentally friendly and cost-effective. Phase transfer with the aid of ODA leads to the nucleation and growth steps occurring within the ODE microdroplets. Balancing the reactivity of metallic cations by adjusting the reaction temperature is a key factor in obtaining single-phase polynary nanocrystals. Furthermore, this approach for the preparation of Cu-based polynary nanocrystals opens a new route for the study and exploitation of other polynary nanocrystals.

Acknowledgments

This work was financially supported by the Chinese Academy of Science Hundred Talents Program and the National Natural Science Foundation of China (nos 10874179 and 60976049). The authors thank Professor Renguo Xie for comments during the manuscript preparation.

References

[1] Habas S E, Platt H A S, van Hest M F A M and Ginley D S 2010 *Chem. Rev.* **110** 6571
[2] Kaneshiro J, Gaillard N, Rocheleau R and Miller E 2010 *Sol. Energy Mater. Sol. Cells* **94** 12
[3] Niki S, Contreras M, Repins I, Powalla M, Kushiya K, Ishizuka S and Matsubara K 2010 *Prog. Photovolt., Res. Appl.* **18** 453
[4] Repins I, Contreras M A, Egaas B, DeHart C, Scharf J, Perkins C L, To B and Noufi R 2008 *Prog. Photovolt., Res. Appl.* **16** 235
[5] Bar M, Repins I, Contreras M A, Weinhardt L, Noufi R and Heske C 2009 *Appl. Phys. Lett.* **95** 052106
[6] Braunger D, Hariskos D, Walter T and Schock H W 1996 *Sol. Energy Mater. Sol. Cells* **40** 97
[7] Klaer J, Siemer K, Luck I and Braunig D 2001 *Thin Solid Films* **387** 169
[8] Katagiri H, Jimbo K, Maw W S, Oishi K, Yamazaki M, Araki H and Takeuchi A 2009 *Thin Solid Films* **517** 2455
[9] Powalla M, Voorwinden G, Hariskos D, Jackson P and Kniese R 2009 *Thin Solid Films* **517** 2111
[10] Jimbo K, Kimura R, Kamimura T, Yamada S, Maw W S, Araki H, Oishi K and Katagiri H 2007 *Thin Solid Films* **515** 599
[11] Kamoun N, Bouzouita H and Rezig B 2007 *Thin Solid Films* **515** 5949
[12] Ahn S, Kim K H, Yun J H and Yoon K H 2009 *J. Appl. Phys.* **105** 133533
[13] Fu Y P, You R W and Lew K K 2009 *J. Electrochem. Soc.* **156** D553
[14] Mitzi D B 2009 *Adv. Mater.* **21** 3141
[15] Todorov T K, Reuter K B and Mitzi D B 2010 *Adv. Mater.* **22** E156
[16] Weil B D, Connor S T and Cui Y 2010 *J. Am. Chem. Soc.* **132** 6642
[17] Guo Q, Ford G M, Yang W C, Walker B C, Stach E A, Hillhouse H W and Agrawal R 2010 *J. Am. Chem. Soc.* **132** 17384
[18] Panthani M G, Akhavan V, Goodfellow B, Schmidtke J P, Dunn L, Dodabalapur A, Barbara P F and Korgel B A 2008 *J. Am. Chem. Soc.* **130** 16770
[19] Norako M E, Franzman M A and Brutchey R L 2009 *Chem. Mater.* **21** 4299
[20] Pan D C, An L J, Sun Z M, Hou W, Yang Y, Yang Z Z and Lu Y F 2008 *J. Am. Chem. Soc.* **130** 5620
[21] Du W M, Qian X F, Yin J and Gong Q 2007 *Chem.—Eur. J.* **13** 8840
[22] Du W M, Qian X F, Ma X D, Gong Q, Cao H L and Yin H 2007 *Chem.—Eur. J.* **13** 3241
[23] Guo Q, Ford G M, Hillhouse H W and Agrawal R 2009 *Nano Lett.* **9** 3060
[24] Shavel A, Arbiol J and Cabot A 2010 *J. Am. Chem. Soc.* **132** 4514
[25] Tang J, Hinds S, Kelley S O and Sargent E H 2008 *Chem. Mater.* **20** 6906
[26] Riha S C, Parkinson B A and Prieto A L 2009 *J. Am. Chem. Soc.* **131** 12054
[27] Guo Q, Hillhouse H W and Agrawal R 2009 *J. Am. Chem. Soc.* **131** 11672
[28] Steinhagen C, Panthani M G, Akhavan V, Goodfellow B, Koo B and Korgel B A 2009 *J. Am. Chem. Soc.* **131** 12554
[29] Dai P, Shen X, Lin Z, Feng Z, Xua H and Zhan J 2010 *Chem. Commun.* **46** 5749
[30] Talapin D V, Lee J S, Kovalenko M V and Shevchenko E V 2010 *Chem. Rev.* **110** 389
[31] Pan D C, Wang Q and An L J 2009 *J. Mater. Chem.* **19** 1063

[32] Dahl J A, Maddux B L S and Hutchison J E 2007 *Chem. Rev.* **107** 2228
[33] Brust M, Walker M, Bethell D, Schiffrin D J and Whyman R 1994 *J. Chem. Soc. Chem. Commun.* 801
[34] Horswell S L, Kiely C J, O'Neil I A and Schiffrin D J 1999 *J. Am. Chem. Soc.* **121** 5573
[35] Pan D C, Zhao N N, Wang Q, Jiang S C, Ji X L and An L J 2005 *Adv. Mater.* **17** 1991
[36] Pan D C, Jiang S C, An L J and Jiang B Z 2004 *Adv. Mater.* **16** 982
[37] Yang J, Sargent E H, Kelley S O and Ying J 2009 *Nat. Mater.* **8** 683
[38] Huang P, Lin J, Li Z, Hu H, Wang K, Gao G, He R and Cui D 2010 *Chem. Commun.* **46** 4800
[39] Fernandes P A, Salomé P M P and da Cunha A F 2009 *Thin Solid Films* **517** 2519
[40] Serrano J, Cantarero A, Cardona M, Garro N, Lauck R, Tallman R E, Ritter T M and Weinstein B A 2004 *Phys. Rev.* B **69** 014301
[41] Xie R, Rutherford M and Peng X 2009 *J. Am. Chem. Soc.* **131** 5691
[42] Tsuji I, Shimodaira Y, Kato H, Kobayashi H and Kudo A 2010 *Chem. Mater.* **22** 1402